Hydroelastic response of submerged wave energy devices†

YongBo Chen, Masoud Hayatdavoodi, and BinBin Zhao

Abstract—**This study is concerned with hydroelastic interaction of water waves with a fully-submerged wave energy device. The oscillating component of the submerged energy device is a circular, horizontal disc. Wave interaction with the horizontal disc results in formation of time-dependent pressure differential above and below the disc, and consequently a periodic vertical force. The wave-induced force on the disc results in vertical oscillations of the horizontal disc. Rigid-body motion of the disc is restricted to vertical oscillations only by use of the guide rails that are attached to the main frame of the energy device, secured on the seafloor. The vertical oscillations of the disc is converted to electricity by use of a direct-drive power take off system. In this study, the effect of wave and structural conditions on the oscillations are studied. The disc may undergo some elastic deformation due to the wave loads, and this may effect the performance of the wave energy device. The hydroelastic deformations of the disc, and its effect on the oscillations is also considered by combining the three-dimensional linear potential theory with the structural finite element analysis. The wave-induced responses of the wave energy device, including oscillations, and structural deformations are presented for a range of wave frequencies, and results are compared with existing laboratory measurements. The elastic deformations are studied for the discs built of different materials and results are compared and discussed. The responses are analyzed for various PTO and control systems.**

Index Terms—**Wave energy device, Wave-structure interaction, Oscillating submerged disc, hydroelasticity**

I. Introduction

Marine renewable energy resources, namely wave energy, current and tidal energy, offshore wind energy, offshore solar, and ocean thermal energy conversion have received significant attention in recent years, see e.g. [1]. Wave energy, when compared to other sources of marine renewable energy, has some distinct advantages including (i) predictability, (ii) highest energy density, and (iii) little energy loss during the wave propagation, see [2]. However, wave energy has not yet been able to provide an economically competitive energy solution. There are several challenges with typical wave energy convertors, including (i) challenges associated to conversion of the wave energy into desirable mechanical energy, (ii) variable wave directions, (iii) large destructive impact of extreme wave loads breaking on devices, (iv) corrosive ocean environment and (v) the undesirable visual impact and the effect on shipping, among others, see e.g. [3], [4]. Hence, simple, directionally invariant, fully submerged devices have received attention in recent years, for example the wave carpet [5], [6], [7], or the oscillating submerged disc device [8], [9].

Oscillating submerged discs are used as (i) the core component of some wave energy devices (see e.g. [8]), (ii) as a wave breaking device in shallow water to mitigate severity of large waves approaching shore lines, (see e.g. [10], [11]), and (iii) as heaving plates in floating offshore structures (see e.g. [12], [13]). The principle behind wave energy devices with a horizontal disc as the prime mover is based on the wave-induced pressure differentials. Wave interaction with submerged horizontal discs causes pressure differential above and below the disc, and hence an oscillatory wave-induced vertical force. If placed on fixed vertical guide rails, the disc oscillates vertically due to the wave-induced force.

Wave-induced vertical oscillations of a submerged disc has been studied by both laboratory experiments and numerical simulation. [14] has conducted a series of laboratory experiments and considered various wave conditions and studied the effect of spring stiffness and initial submergence on the disc oscillations. Following the approached presented by [15] for nonlinear wave loads on a submerged plate, oscillations of a horizontal submerged plate was studied by use of the Level I Green-Naghdi equations in [9]. [11] has studied a submerged heaving plate as a breakwater by using a nonlinear potential theory solver. Their results show that the heaving plate can significantly decrease the energy transmission at a certain condition compared with the fixed one. In a study performed by [16] based on the weakly compressible particle hydrodynamics method, application of a submerged disc in a wave energy system is further analyzed. Computational fluid dynamics method is used by

†The 14th European Wave and Tidal Energy Conference, EWTEC2021, 5-9 September, 2021, Plymouth, UK.
Paper ID:1966. Track: Wave hydrodynamic modelling

Y.B. Chen is with the college of shipbuilding Engineering, Harbin Engineering University, Harbin, China (e-mail: chenyongbo@hrbeu.edu.cn).

M. Hayatdavoodi is with the Marine Hydrodynamics and Ocean Engineering of Civil Engineering Department, School of Science and Engineering, University of Dundee, Dundee, DD1 4HN, UK (e-mail: MHayatdavoodi@dundee.ac.uk).

B.B. Zhao is with the college of shipbuilding Engineering, Harbin Engineering University, Harbin, China (e-mail: zhaobinbin@hrbeu.edu.cn).

[17], which shows the submerged heaving plate breakwater works better around short and medium wavelengths.

While analysis of energy production from an oscillation disc is a challenging problem in hydrodynamics, of course structural considerations should also be included which add to the complexity of the problem. In particular, a horizontal disc is subject to deformations and hence hydroelastic analysis is required.

Hydroelasticity is often used to determine the deformations of marine structures subject to wave loads, and is particularly important when load frequencies are close to the natural frequencies of the structure. A general review of the hydroelasticity theory and applications can be found in [18]. Hydroelasticity has been an integrated part of design and analysis of wave energy systems. For example, [19] uses a semi-analytical approach to study the piezoelectric wave energy converter, a submerged elastic plate, whose leading and trailing edges are fixed. [20] has developed a linear numerical model to study an elastic wave energy converter, consisting of a submerged elastic horizontal tube with pressurized water inside the device. Wave-induced elastic response of a flexible submerged horizontal porous plate is studied by [21] and [22] by use of the linear potential theory coupled with a matched eigenfunction expansion. The wave induced elastic response of a single, submerged porous disc and an array of discs is also studied by [23]. By coupling computational fluid dynamics with finite element method, [24] investigates the interaction of a solitary wave with a submerged elastic upper plate. Nonlinear wave-induced deformations of fixed submerged horizontal discs made of different material are studied by [25], where the wave loads are determined by the Level I Green-Naghdi equations and the response of the elastic disc is obtained by use of the finite element method. See [26] for nonlinear wave interaction with elastic plates on the free surface by the Green-Naghdi equations.

Here, hydroelastic analysis of a submerged horizontal heaving horizontal disc attached to a control and power take-off system for energy production is studied by use of the linear wave theory for the fluid motion, coupled with the mode-shape analysis for the structural consideration. In section III, the rigid body motions and hydroelastic theories are introduced. Numerical results are presented and discussed in section IV. The paper is closed with concluding remarks in section V.

II. SWED: The Submerged Wave Energy Device

The fully submerged wave energy device under consideration in this study (SWED) is proposed and developed as an oscillating circular disc with a fixed frame sitting on the seafloor. Wave pressure differential above and below the disc results in its vertical oscillations. The prime mover is restricted to only vertical oscillations, and horizontal and rotational motions are restricted by use of vertical guided rails. The device benefits from the circular shape of the prime mover whose oscillation is invariant with wave propagation direction. More details about SWED can be found in [8], [14], [25] and [27].

In this study, a spring is attached to the disc to contribute to the motion control of the device. The spring modifies the wave-induced motions, as well as avoid the disc from moving towards the free surface or the seafloor. The spring stiffness affects the response of the disc and understanding the behaviour of the disc under different springs is one of the objectives of this study.

A direct-drive power take-off (PTO) system, located on the sea floor, is connected to the disc to convert the mechanical motion to electricity. The PTO system is designed as a linear generator including an air-cored ferromagnetic translator and a stationary stator. The translator is linked to the bottom face of the disc by a solid shaft. The effect of the PTO system on the motion is similar to viscous damper, resisting against the motion of the disc proportional to its velocity. The effect of various PTO damping on the motion of the disc will be analysed in this study. A schematic of the energy device and the domain is shown in Fig. 1.

Various parameters influence the power output of SWED. These include the wave conditions (wave period and wave height), initial submergence depth of the disc, the spring stiffness, the PTO damping coefficient, and disc material (mass and density) and deformations, among others. The response of the device under these variables will be studied here. Throughout this paper, the water depth where the device is located at, is constant.

III. Theory

Wave-induced vertical oscillations of rigid and flexible submerged horizontal discs are considered. The fluid is incompressible and inviscid. The flow is irrotational at the invariant water depth. Fluid's velocity potential satisfies Laplace's equation throughout the entire fluid domain and the incoming waves are regular and long-crested. Under this frame work, the linear hydrodynamics theory, combined with the green function and constant panel methods, is used to obtain the frequency domain solutions of wave interaction with the oscillating disc, see e.g. [28], [29] and [30]. The linear structural dynamics behavior is considered to solve elastic responses of the disc based on assumed modes approach. In this study, a right-hand Cartesian coordinate system is used, whose origin is on the water level, with X_1 pointing to the right, X_2 pointing upwards and X_3 pointing into the page.

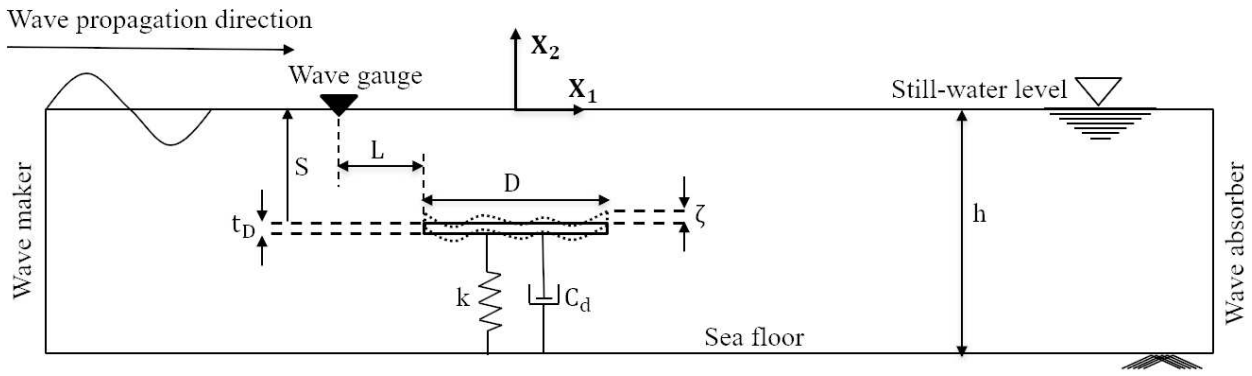

Fig. 1: Two dimensional schematic of wave interaction with the submerged wave energy device. D is the diameter of the disc, t_D is its thickness, S is the instantaneous submergence depth, measured from the top surface of the (rigid) plate to the SWL, ζ is the deformation amplitude of the disc at a given point and $h = 0.3$ m is the constant water depth in this study. L is the distance between the wave gauge and the leading edge of the circular disc.

A. Rigid body hydrodynamics

Linear potential theory is used to study the wave-induced vertical oscillations of a submerged horizontal disc. In this approach, the total velocity potential is decomposed into incoming potential, diffraction potential, and radiation potentials due to the motion of the body. All potentials satisfy Laplace's equation, the linear free surface boundary conditions and the no-flux condition on the seafloor, and the body boundary condition. The diffraction and radiation potentials also satisfy the radiation condition. Solution of the velocity potentials is obtained by use of the Green function and panel method.

Once the velocity potentials are obtained, the hydrodynamic pressure can be determined by use of Euler's integral. The total force on the body consists of the wave exciting force (due to the incoming wave potential and diffraction potential), the hydrostatic forces, and the hydrodynamic radiation forces (consisting of the added mass and wave-damping forces). See [28], [29] among other for details.

The equation of motion of the vertically oscillating body is then obtained by substituting the involved forces into Newton's second law and it reads as

$$(m_s + m_f)\ddot{x}_2 + (c_f + C_d)\dot{x}_2 + kx_2 = \sum F_2, \quad (1)$$

where $\ddot{x}_2, \dot{x}_2$ and x_2 are the vertical acceleration, velocity and displacement of the disc, respectively, m_s is the mass of the disc, and m_f and c_f are the added mass and hydrodynamic damping coefficients, respectively. Note that the oscillations start from an equilibrium position and hence static forces (weight and buoyancy) do not play a role on the oscillations. The external spring force is $-kx_2$, where x_2 is measured from the initial equilibrium position of the disc, and k is the spring stiffness. The damping force is $-C_d\dot{x}_2$, resembling the effect of the PTO system, if used, and C_d is the constant damping coefficient. The sum of other vertical external forces, $\sum F_2$ on the right hand side of Eq. (1) are given as

$$\sum F_2 = F_{w_2} + F_f, \quad (2)$$

where F_{w_2} is the vertical component of the wave-exciting force, and F_f is the friction force between the disc and the guide rails, defined as $F_f = -\mu F_{w_1}$, where μ is the constant friction coefficient. F_{w_1} is the horizontal component of the wave-exciting force on the disc.

In the linear theory, the displacement x_2 (and consequently velocity and acceleration) and the wave-exciting force F_w are harmonic functions with frequency ω. Substituting $x_2 = x_0 e^{i\omega t}$ and $F_{w_2} = AF_0 e^{i\omega t}$ into Eq. (1), where A is the wave amplitude and F_0 is the exciting wave force per unit wave amplitude, the linear equation of motion of the disc is given by

$$(-\omega^2(m_s + m_f) + i\omega(c_f + C_d) + k)x_0 = AF_0. \quad (3)$$

Solving (3) will give the transfer function x_0/A, which is the square root of the response amplitude operator (RAO) of the vertical displacement of the disc, in frequency domain.

B. Hydroelastic analysis

Wave loads may cause disc's elastic deformations when incoming wave frequencies are close to the natural frequencies of the elastic disc. The elastic responses may alter device's hydrodynamic performance. To study this, linear hydroelasticity is used here by coupling the finite element mesh of the structure and the panel mesh of the fluid-structure interface. Disc's displacement in the frequency domain solution is obtained by solving the linear equation of motion based on the mode shape

method. The mode shape of the disc is formed through the finite element model, see [31], [32] for details.

Motion of the disc is limited to only one degree of freedom in rigid case where its displacement is $x_2 = x_0 e^{i\omega t}$. In total, there are N degrees of freedom for the oscillations of the elastic disc, whose displacement $u(X_1, X_2, X_3, t)$

$$u = u_0 e^{i\omega t}, \tag{4}$$

where u_0 is the $N \times 1$ vector of the displacement amplitude of the elastic disc.

The assumed mode method is used to determine the displacement of the elastic disc. In this approach, for the disc with N degrees of freedom, its displacement u is represented by the summation of each mode vector where $u(X_1, X_2, X_3, t) = \sum_{j=1}^{N} \psi_j(X_1, X_2, X_3) Y_j(t)$, where $Y_j(t)$ is the non-dimensional generalized coordinate of mode shape $\psi_j(X_1, X_2, X_3)$. This can be written as

$$u = \psi Y, \tag{5}$$

where ψ is the $N \times N$ modal matrix; hence, ψ_j is the mode vector forming the j^{th} column of the mode matrix ψ. Y is a $N \times 1$ vector whose first row is Y_1, i.e. N^{th} row is Y_N.

The modes basis can be obtained by solving the undamped free-vibration equation, given as

$$[K_s - \omega_j^2 M_s]\psi_j = O, \quad j = 1, 2, ..., N \tag{6}$$

where M_s is the structural mass of the disc, K_s is the structural stiffness of the disc. Both M_s and K_s are $N \times N$ matrices. ω_j is the j^{th} natural circular frequency of the elastic disc.

The following orthogonal restrictions are used to obtain the unique mode shapes through Eq. (6).

$$\psi_j^T K_s \psi_q = \begin{cases} \omega_j^2, & j = q, \\ 0, & j \neq q, \end{cases} \tag{7a}$$

$$\psi_j^T M_s \psi_q = \begin{cases} 1, & j = q, \\ 0, & j \neq q. \end{cases} \tag{7b}$$

The equation of motion of the elastic disc with N degree of freedom including the radiation force, wave exciting force and the associated spring, damper and friction force, is formulated as

$$(-\omega^2(M_s+M_f)+i\omega(C_s+C_f)+(K_s+K_f+K_{ex}))u = F_f, \tag{8}$$

where C_s is the $N \times N$ structural damping matrix of the disc. M_f is the $N \times N$ added mass matrix, C_f is the $N \times N$ hydrodynamic damping matrix, K_f is the $N \times N$ hydrostatic matrix and K_{ex} is the $N \times N$ stiffness matrix of the external spring force. F_f is the $N \times 1$ wave exciting force vector. K_{ex} is specified depends on needs. C_s and K_f are not included in this study.

Substituting (5) into (8), then multiplying by ψ^T forms

$$(-\omega^2(M_s^* + M_f^*) + i\omega C_f^* + (K_s^* + K_{ex}^*))Y = F_f^*, \tag{9}$$

where $M_s^* = \psi^T M_s \psi$ is the identity matrix, $K_s^* = \psi^T K_s \psi$ is a diagonal matrix whose diagonal component is equal to the square of natural frequencies. $M_f^* = \psi^T M_f \psi$, $C_f^* = \psi^T C_f \psi$, $K_{ex}^* = \psi^T K_{ex} \psi$, and $F_f^* = \psi^T F_f$. These are obtained after calculating the hydrodynamic parameters for each mode shape.

A reduced strategy of M (where $M << N$) total modes is used in this study, see [32]. That is the displacement u of the elastic disc is approximated by

$$u \approx \psi_{NM} Y_M, \tag{10}$$

where ψ_{NM} is a $N \times M$ modal matrix and Y_M is a $M \times 1$ vector. Substituting (10) to (9), Y_M can be calculated, and then the displacement of elastic disc under wave frequency ω is approximately estimated by (10).

Computation of linear wave interaction with the elastic disc are carried out in HYDRAN-XR. See [33], [31], [34], [35], [36], and more recently in [37], for more details about the hydroelastic model used in this study.

IV. Results & Discussions

Linear theory is used to study the wave interaction with a fully submerged rigid and elastic disc. A two dimensional schematic of the domain is shown in Fig. 1, showing the involved parameters. Results are first compared with the laboratory measurements of [14]. This is then followed by discussion on the effect of various parameters and the responses. In this study, the friction force F_f is not considered, although this is not required in general. The effect of the friction between the disc and the guide rails can be included, see [8], but this is negligible when compared to other forces. In all cases considered, there is a spring attached to the disc. Limited cases, also include the viscous damper and these are clearly stated. Initially, all results are given for the rigid disc, followed by a section where hydroelastic analysis is presented. Unless otherwise stated, dimensions of the disc of the laboratory measurements of [14] is used in the analysis. Unless otherwise stated clearly in subsection, no damping (resembling the PTO effect) is used in obtaining the results presented here.

A. Comparisons with laboratory experiment

The laboratory experiments of [14] are used for the comparison purpose. The experiments were conducted in the Fluid Mechanics laboratory of the University of Dundee, UK, in constant water depth of $h = 0.3$ m. One wave gauge is placed upwave from the disc to record the surface elevation, whose location is shown in Fig. 1. A circular disc with diameter $D = 0.3$ m and thickness of $t_D = 3$ mm is used in the experiments. The mass of the circular disc (along with the attached linear bearing and the

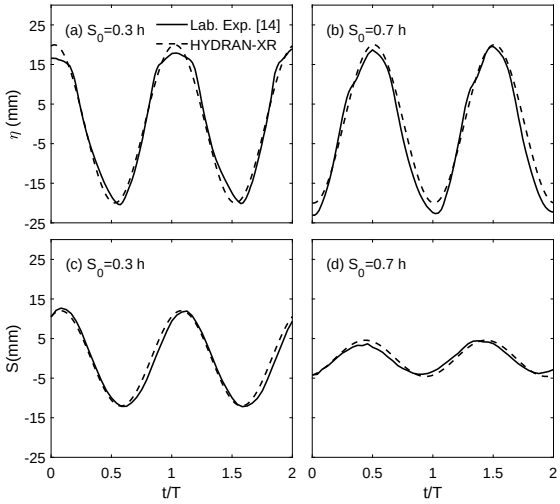

Fig. 2: Comparisons of time series of disc's vertical oscillations (S) and wave surface elevation (η) of the laboratory experiments of [14] and numerical results of this study (HYDRAN-XR). $k = 35.7$ N/m, wave period $T = 1$ s, wave height $H = 4$ cm and water depth $h = 0.3$ m. The surface elevation (η) is recorded by the wave gauge located at the upwave position, $L = 0.6$ m far away from the leading edge of the disc.

connecting screws in the laboratory experiments) is 432 g. See [14] for more details about the experiments, the specimen, and the setup of the tests.

Figure 2 shows comparison of time series of disc's oscillation (S) and wave surface elevation (η) between laboratory measurements and numerical results for two cases of different initial submergence depths, S_0 (defined as the initial distance from the still-water level to the top of the disc). The disc oscillates with the same period as the wave, and this is not remarkable. The amplitude of the oscillations varies with the initial submergence depth of the disc. Oscillations of the disc is significantly larger at the $S_0 = 0.3\ h$. Overall, very good agreement is observed between the numerical results of this study and the laboratory measurements of this study.

B. Effect of the initial submergence depth

Figure 3 shows the heave RAO of the submerged disc for four initial submergence depths and two spring stiffness. Shown in Fig. 3, the amplitude of the vertical oscillations vary nonlinearly with the wave period. Initial submergence depth has inverse effect on the oscillations, that is, oscillations' amplitude decreases with the increasing submergence depth. The variation appears to be nonlinear. Note that the laboratory experiments of [14] are conducted for various wave heights. In Fig. 3, results of the experiments (vertical oscillations) are normalized by wave amplitude (to obtain the heave RAO) and used for comparison with HYDRAN-XR results. Overall, good agreement is observed between results of the linear theory and the laboratory experiments. The agreement is better for shorter waves, with some deviations between the results when the wave period increases. In this case, the oscillation heave RAOs tend to one for larger wave periods. The effect of the spring on the disc oscillations is not remarkable in most of the cases considered in Fig. 3. This, however, is not always the case and hence, in the next section, we study the effect of the spring stiffness on the disc oscillations.

C. Effect of the springs

It is desirable to optimize the system for largest oscillations of the disc (and ultimately for maximum power output). Shown in Fig. 4, we study the change in oscillations' amplitude with the spring stiffness for a given wavelength ($\lambda/D = 2$, where λ is the wavelength). For all four submergence depths, a clear peak of the oscillations is observed. Shown in Fig. 4, with the increasing submergence depth, the peak of the oscillations occurs at larger stiffness, and its magnitude increases (it is larger than 1 for $S_0 = 0.5$ and 0.7). This is due to the change in the wave-induced force on the submerged disc at larger depths. See e.g. [38], [39] for the effect of change in submergence depth on the wave-induced loads on a submerged plate. In general, in forced oscillations, and as shown in [40], the point of resonance varies with the change of the external force and the spring stiffness, among other parameters. Here, the change of the wave-induced force on the disc with larger submergence depth is such that the peak of the oscillations occurs when the spring stiffness is larger. To better study the effect of the spring force on the oscillations, we consider four different spring stiffness (including one with $k = 0$, i.e. no spring effect) and obtain the results through the linear solver. The heave RAOs are shown in Fig. 5 for four submergence depths. The variation of the oscillation amplitudes with spring stiffness is nonlinear at different submergence depths. For the case of no spring, the amplitude of the disc oscillations converges to a fixed value (at periods about $T = 1$ s in this particular case), and then remains invariant. This is because the wave-induced loads on a submerged disc becomes invariant of the wave period (or wavelength), when the ratio of the wavelength to disc diameter exceeds a threshold (see [41] and [39]). Stronger springs seem to decrease the structure's natural periods where resonance happens.

D. Effect of disc diameter

Shown in Fig. 6, the ratio of wavelength to disc diameter λ/D plays a significant role on the disc oscillations for all submergence depths. Oscillations are remarkably smaller at $\lambda/D < 1$ i.e. when there are multiple waves on the disc at the same time, and

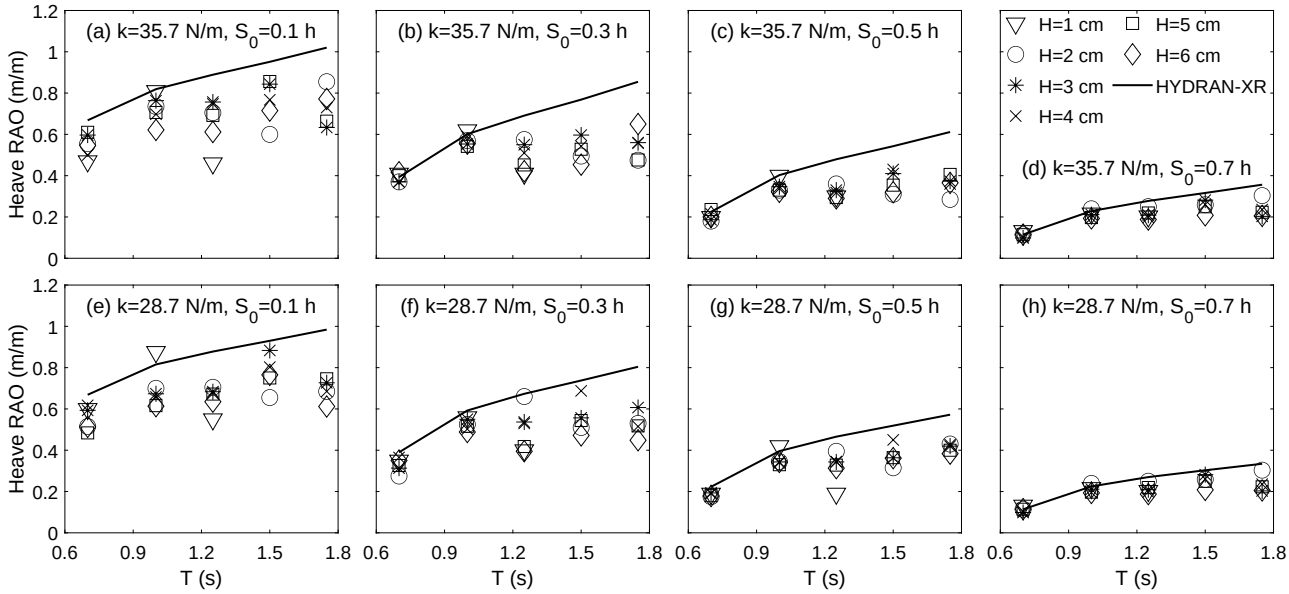

Fig. 3: Comparisons of the heave RAOs of the submerged disc obtained by the laboratory experiments of [14] and numerical results of this study (HYDRAN-XR) of the submerged disc for four submergence depths. Markers refer to the laboratory experiment results, and H is incident wave height.

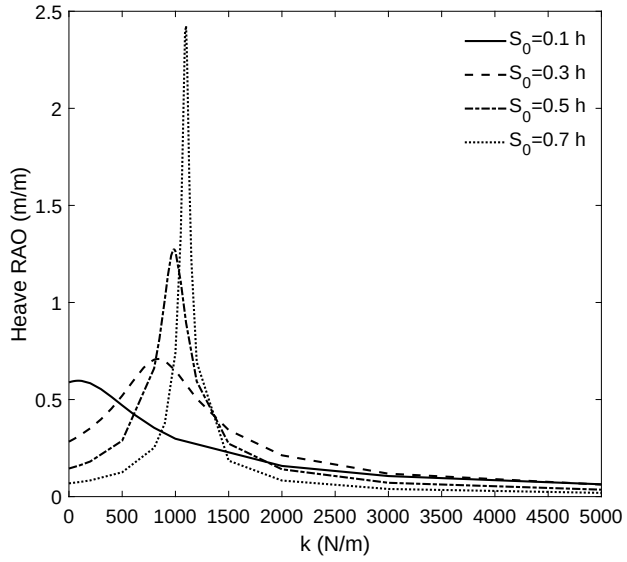

Fig. 4: Variation of the heave oscillations with the spring stiffness at different submergence depths, and for a constant wavelength ($\lambda/D = 2$).

this is expected. This is due to the significant effect of the λ/D ratio on the wave-induced forces on the disc. For $\lambda/D < 1$, multiple waves are in contact with the disc at the same time, and their downward and upward forces may interfere with each other simultaneously. For cases where the wavelength and disc diameter are comparable, at a given time, only one wave is in contact with the disc and the uplift and downward forces vary depending on the lengths ratio (whether wave crest or trough are in touch with the disc simultaneously or not). For long waves where the wavelength is significantly larger than the disc diameter, the object is almost like a particle. See [41] for discussion on the variation of the forces with wavelength to disc diameter ratio.

E. Effect of PTO

The vertical oscillation of the horizontal disc is converted to electricity by use of a direct-drive PTO system. The PTO affects the oscillations similar to a damper. To study the PTO effect, in this section we consider the wave induced oscillations of the disc under the influence of different PTO strengths (i.e. different damping coefficients).

The results are shown in Fig. 7. The effect of damping force on oscillations of the disc are studied for four different submergence depths. It is observed that the damping coefficient C_d has a reverse influence on oscillations of the disc. The maximum oscillations of the disc are reduced significantly when $C_d = 40$ Ns/m and $C_d = 100$ Ns/m, with very small oscillation under the damping coefficient $C_d = 100$ Ns/m and initial submergence $S_0 = 0.7\ h$.

F. Effect of elastic deformations

In this section, we shall study the elastic deformations of the submerged disc due to the wave loads. For this hydroelastic analysis, we consider a circular disc with the same geometry and mass discussed in the previous sections. The mass density of the disc is 2037 Kg/m^3, with Young's modulus and Poisson's ratio of $1.5E+10$ Pa and 0.3, respectively. The flexible disc undergos vertical rigid-body oscillations

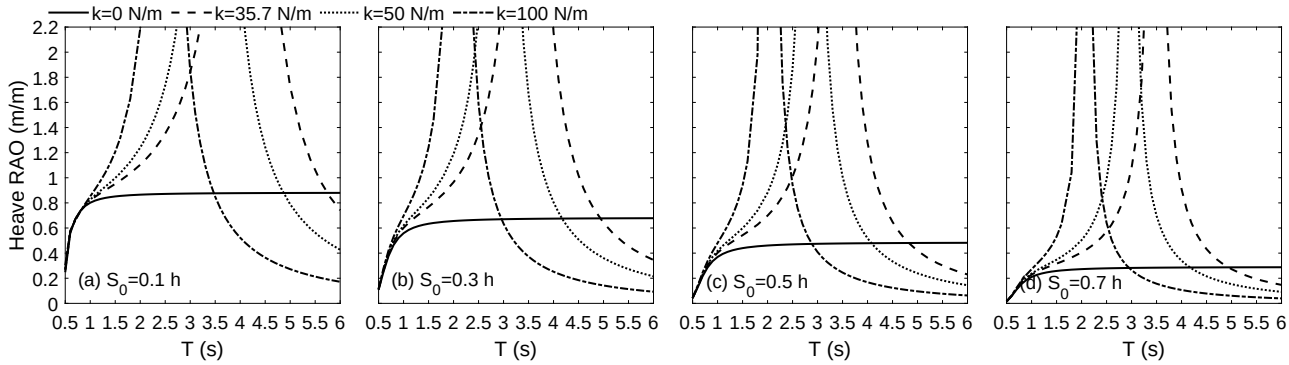

Fig. 5: Variation of the heave oscillations with spring stiffness at different submergence depths.

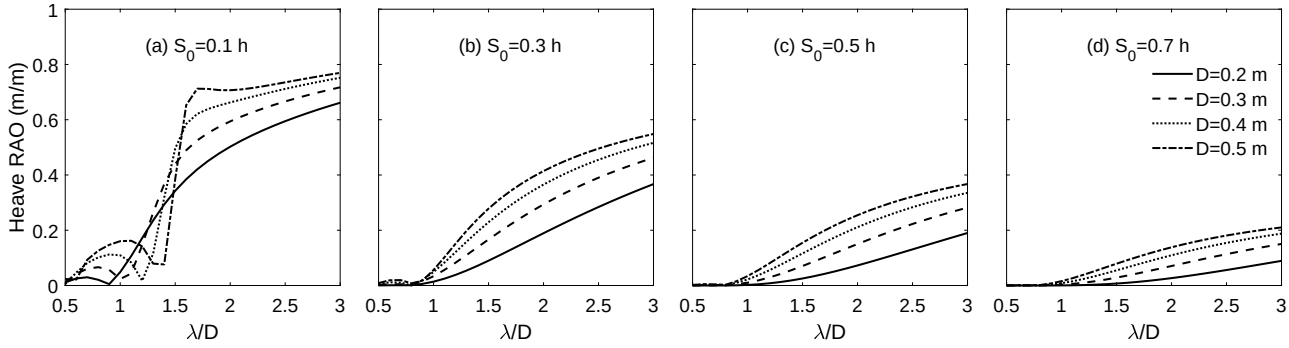

Fig. 6: Variation of the heave oscillations with λ/D at different submergence depths($k = 35.7$ N/m).

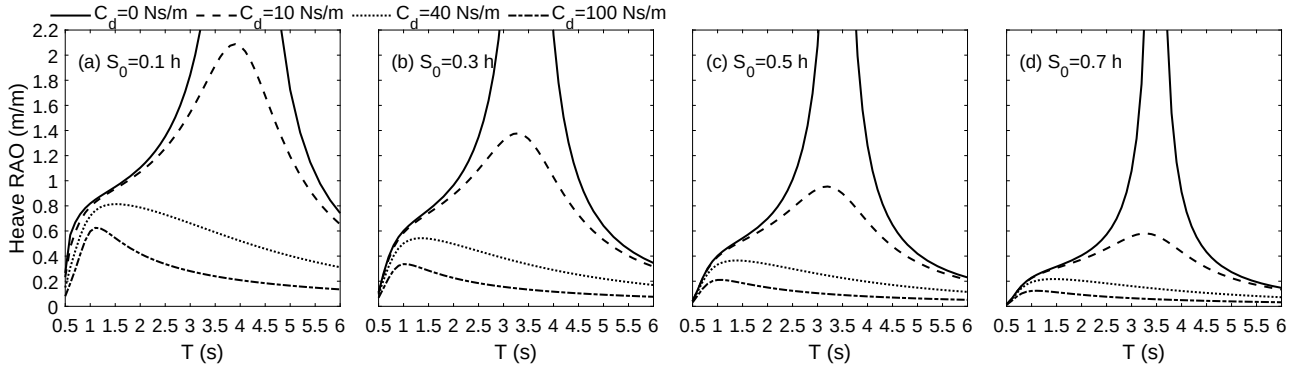

Fig. 7: Variation of the heave oscillations with damping coefficient C_d at different submergence depths ($k = 35.7$ N/m).

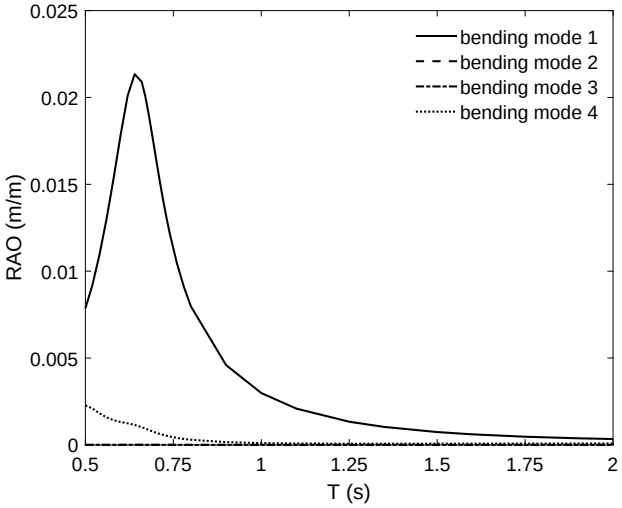

Fig. 8: RAOs of the first four bending mode of the disc ($k = 35.7$ N/m).

TABLE I:
MATERIAL PROPERTY.

	Concrete	Aluminium	Titanium	Steel
ρ(kg/m^3)	2300	2770	4620	7750
E(Pa)	3.00E+10	7.10E+10	9.60E+10	1.93E+11
ν	0.18	0.33	0.36	0.31

as well as vertical bending deformations. In total, 12 modes including 1 rigid mode and 11 flexible bending modes are adopted in this study. RAOs of the first four bending modes of the elastic disc are shown in Fig. 8. Bending mode 1 contributes more significantly to disc's bending RAO, shown in Fig. 8. This is substantially smaller than the rigid-body vertical oscillations as expected.

In practice, the disc may be built of different materials, and the responses of the elastic discs made of different materials vary under the same wave loads. Here, the deformation magnitude of the elastic discs made of concrete, aluminium alloy, titanium and steel, is studied for different submergence depths. Their material properties are listed in Table I where E is Young's modulus and ν is Poisson's ratio.

Shown in Fig. 9, the maximum deformations of the elastic circular disc at leading edge point vary with incoming wave frequency at different initial submergence depths. The results show increasing submergence depth affects the elastic disc's response inversely. It is also observed that the elasticity properties of the disc have little effect under waves with larger periods. This can be also seen in Fig. 10, which shows the spatial distributions of the elastic disc's maximum deformations at the initial submergence of $S_0 = 0.1\ h$ for four different wave frequencies. Comparing with other materials, concrete shows the largest deformations followed by aluminium, titanium and steel.

V. CONCLUDING REMARKS

Wave-induced responses of a fully-submerged oscillating horizontal disc is studied numerically by using the linear theory. Both rigid and elastic responses are considered in this study.

Vertical oscillations are first studied by comparing with the laboratory measurements. Numerical results show excellent agreement with shorter waves. The model is then used to analyse the responses of the device under various wave and structural conditions.

The oscillations decrease with increasing submergence depth due to smaller hydrodynamic pressure differentials. The spring generally has a nonlinear influence on disc's oscillations. The damping force affects the maximum oscillations adversely. The oscillations of the disc are reduced significantly with a large damping coefficient for different submergence depths.

The ratio of wavelength to disc diameter λ/D is extended further by changing disc's diameter. This is of importance to disc's oscillation amplitude for all submergence depths. Oscillations are significantly smaller at $\lambda/D < 1$.

Linear hydroelasticity is also used to study hydroelastic response of the disc. One rigid mode and eleven flexible modes are adopted to account for vertical oscillations and bending deformations, respectively. The disc deforms much more significantly under shorter waves and the elastic response are negligible for longer incoming waves. The elastic response of the disc made of four different materials are considered including concrete, aluminium, titanium and steel. The leading and trailing edge of the disc undergo largest structural deformations, and this is not remarkable. Concrete has the largest elastic deformations while the steel is inactive for various wave frequencies.

ACKNOWLEDGEMENTS

The authors are grateful to Professor H. Ronald Riggs of the University of Hawaii for the invaluable advice and support on adopting HYDRAN-XR for this study.

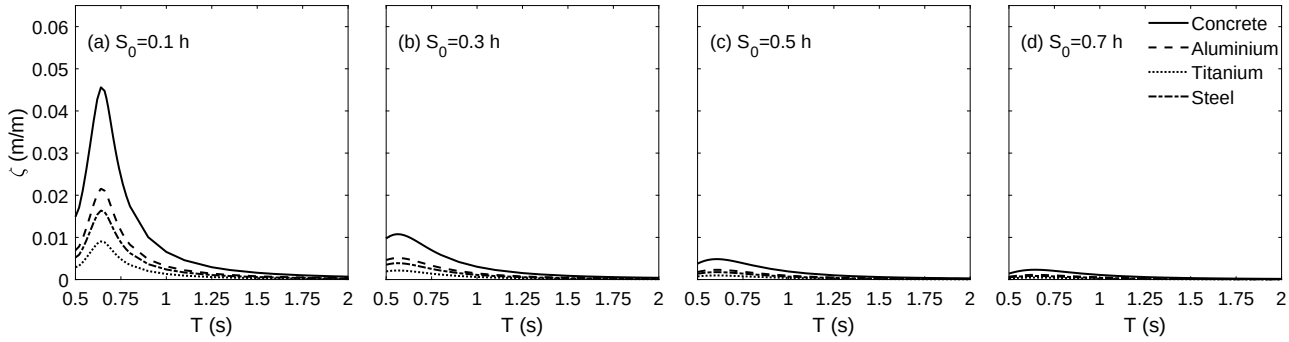

Fig. 9: Deformation amplitude of the leading edge point of the elastic disc made of four different materials, and initially submerged at different depths. ($k = 35.7$ N/m)

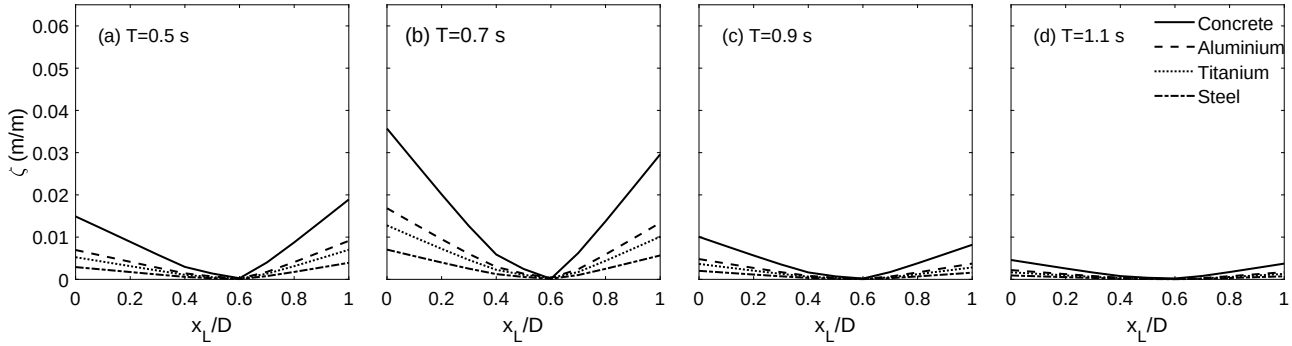

Fig. 10: Spatial distributions of elastic disc's maximum deformation made of four different materials under five different wave periods at the initial submergence depth of $S_0 = 0.1\ h$. ($x_L = 0$ is corresponding to the leading edge, $k = 35.7$ N/m)

References

[1] A. Day, A. Babarit, A. Fontaine, Y.-P. He, M. Kraskowski, M. Murai, I. Penesis, F. Salvatore, and H.-K. Shin, "Hydrodynamic modelling of marine renewable energy devices: A state of the art review," *Ocean Engineering*, vol. 108, pp. 46–69, 2015.

[2] S. Jin and D. Greaves, "Wave energy in the uk: Status review and future perspectives," *Renewable and Sustainable Energy Reviews*, vol. 143, p. 110932, 2021.

[3] S. Astariz and G. Iglesias, "The economics of wave energy: A review," *Renewable and Sustainable Energy Reviews*, vol. 45, pp. 397–408, 2015.

[4] Y. Zhang, Y. Zhao, W. Sun, and J. Li, "Ocean wave energy converters: Technical principle, device realization, and performance evaluation," *Renewable and Sustainable Energy Reviews*, vol. 141, p. 110764, 2021.

[5] M.-R. Alam, "Nonlinear analysis of an actuated seafloor-mounted carpet for a high-performance wave energy extraction," *Proceedings of the Royal Society A: Mathematical, Physical and Engineering Sciences*, vol. 468, no. 2146, pp. 3153–3171, 2012.

[6] M. Lehman, R. Elandt, M. Shakeri, and M.-R. Alam, "The wave carpet: Development of a submerged pressure differential wave energy converter," in *Proceedings of the 30th Symposium on Naval Hydrodynamics, Hobart, Australia, 2-7 Novembe*, 2014.

[7] M. Hayatdavoodi and R. C. Ertekin, "Hydroelastic response of a submerged plate to long waves," in *32nd International Workshop On Water Waves And Floating Bodies (IWWWFB32), Dalian, China*, 2017, pp. 23–26.

[8] M. Hayatdavoodi, R. C. Ertekin, and J. T. Thies, "Conceptual design and analysis of a submerged wave energy device in shallow water," in *International Conference on Offshore Mechanics and Arctic Engineering, OMAE2017, June 25-30, Trondheim, Norway*, vol. 57786, 2017, p. V010T09A033.

[9] M. Hayatdavoodi, J. Wagner, J. Wagner, and R. C. Ertekin, "Vertical oscillation of a horizontal submerged plate," in *31st International Workshop on Water Waves and Floating Bodies (IWWWFB)*, 2016, pp. 1–4.

[10] M. Hayatdavoodi, R. C. Ertekin, and B. D. Valentine, "Solitary and cnoidal wave scattering by a submerged horizontal plate in shallow water," *AIP Advances*, vol. 7, no. 6, p. 065212, 2017.

[11] C. Liu, Z. Huang, and W. Chen, "A numerical study of a submerged horizontal heaving plate as a breakwater," *Journal of Coastal Research*, vol. 33, no. 4, pp. 917–930, 2017.

[12] H.-J. Koh and I.-H. Cho, "Heave motion response of a circular cylinder with the dual damping plates," *Ocean Engineering*, vol. 125, pp. 95–102, 2016.

[13] A. Brown, J. Thomson, and C. Rusch, "Hydrodynamic coefficients of heave plates, with application to wave energy conversion," *IEEE Journal of Oceanic Engineering*, vol. 43, no. 4, pp. 983–996, 2017.

[14] L. Eckel and M. Hayatdavoodi, "Laboratory experiments of wave interaction with submerged oscillating bodies," in *Proc. The 13th European Wave and Tidal Energy Conference, EWTEC2019, 1-6 September, Napoli, Italy*, 2019, pp. 1–9.

[15] M. Hayatdavoodi and R. C. Ertekin, "Wave forces on a submerged horizontal plate. part I: Theory and modelling," *Journal of Fluids and Structures*, vol. 54, pp. 566–579, 2015.

[16] M. He, X. Gao, W. Xu, B. Ren, and H. Wang, "Potential application of submerged horizontal plate as a wave energy breakwater: A 2d study using the wcsph method," *Ocean Engineering*, vol. 185, pp. 27–46, 2019.

[17] D. Fu, X. Zhao, S. Wang, and D. Yan, "Numerical study on the wave dissipating performance of a submerged heaving plate breakwater," *Ocean Engineering*, vol. 219, p. 108310, 2021.

[18] X.-j. Chen, Y.-s. Wu, W.-c. Cui, and J. J. Jensen, "Review of hydroelasticity theories for global response of marine structures," *Ocean Engineering*, vol. 33, no. 3-4, pp. 439–457, 2006.

[19] E. Renzi, "Hydroelectromechanical modelling of a piezoelectric wave energy converter," *Proceedings of the Royal Society A: Mathematical, Physical and Engineering Sciences*, vol. 472, no. 2195, p. 20160715, 2016.

[20] A. Babarit, J. Singh, C. Mélis, A. Wattez, and P. Jean, "A linear numerical model for analysing the hydroelastic response of a flexible electroactive wave energy converter," *Journal of Fluids and Structures*, vol. 74, pp. 356–384, 2017.

[21] S. C. Mohapatra and C. G. Soares, "Hydroelastic response of a flexible submerged porous plate for wave energy absorption," *Journal of Marine Science and Engineering*, vol. 8, no. 9, p. 698, 2020.

[22] S. Mohapatra and C. G. Soares, "Hydroelastic behaviour of a submerged horizontal flexible porous structure in three-dimensions," *Journal of Fluids and Structures*, vol. 104, p. 103319, 2021.

[23] S. Zheng, M. Meylan, D. Greaves, and G. Iglesias, "Water-wave interaction with submerged porous elastic disks," *Physics of Fluids*, vol. 32, no. 4, p. 047106, 2020.

[24] Z. Hu, X. Zhang, Y. Li, X. Li, and H. Qin, "Numerical study on hydroelastic interaction between solitary wave and submerged box," *Ocean Engineering*, vol. 205, p. 107299, 2020.

[25] S. Li, M. Hayatdavoodi, and R. C. Ertekin, "On wave-induced elastic deformations of a submerged wave energy device," *Journal of Marine Science and Application*, vol. 19, no. 3, pp. 317–338, 2020.

[26] V. Kostikov, M. Hayatdavoodi, and R. C. Ertekin, "Hydroelastic interaction of nonlinear waves with floating sheets," *Theoretical and Computational Fluid Dynamics*, pp. 1–23, DOI: 10.1007/s00 162–021–00 571–1., 2021.

[27] J. J. Wagner, J. R. Wagner, and M. Hayatdavoodi, "Hydrodynamic analysis of a submerged wave energy converter," in *Proc. 4th Marine Energy Technology Symposium, METS2016, Washington, DC, USA, April 25-27, 5 p*, 2016.

[28] J. N. Newman, *Marine hydrodynamics*. The MIT press, 2018.

[29] O. Faltinsen, *Sea loads on ships and offshore structures*. Cambridge university press, 1993, vol. 1.

[30] D. Wang, R. C. Ertekin, and H. R. Riggs, "Three-dimensional hydroelastic response of a very large floating structure," *International Journal of Offshore and Polar Engineering*, vol. 1, no. 04, 1991.

[31] R. C. Ertekin, H. R. Riggs, X. Che, and S. Du, "Efficient methods for hydroelastic analysis of very large floating structures," *Journal of Ship Research*, vol. 37, no. 01, pp. 58–76, 1993.

[32] H. R. Riggs and S. Yim, "Structural dynamics," in *Springer Handbook of Ocean Engineering, Edts. Dhanak, M. R. and Xiros, N. I.* Springer International Publishing, 2016, pp. 851–874.

[33] D. Wang, R. C. Ertekin, and H. R. Riggs, "Three-dimensional hydroelastic response of a very large floating structure," *International Journal of Offshore and Polar Engineering*, vol. 1, no. 04, 1991.

[34] H. R. Riggs, R. C. Ertekin, and T. R. J. Mills, "Wave-induced response of a 5-module mobile offshore base," in *17th International Conference on Offshore Mechanics and Arctic Engineering, Lisbon, Portugal*, 1998.

[35] Riggs, H. R. and Ertekin, R. C. and Mills, T. R. J. , "Impact of connector stiffness on the response of a multi-module mobile offshore base," in *The Eighth International Offshore and Polar Engineering Conference, May 24-29, Montreal, Canada*. International Society of Offshore and Polar Engineers, 1998.

[36] L. L. Huang and H. R. Riggs, "The hydrostatic stiffness of flexible floating structures for linear hydroelasticity," *Marine Structures*, vol. 13, pp. 91–106, 2000.

[37] H. R. Riggs, K. M. Niimi, and L. L. Huang, "Two benchmark problems for three-dimensional, linear hydroelasticity," *Journal of Offshore Mechanics and Arctic Engineering*, vol. 129, no. 3, pp. 149–157, 2007.

[38] M. Hayatdavoodi and R. C. Ertekin, "Wave forces on a submerged horizontal plate. part II: Solitary and cnoidal waves," *Journal of Fluids and Structures*, vol. 54, pp. 580–596, 2015.

[39] M. Hayatdavoodi, K. Treichel, and R. C. Ertekin, "Parametric study of nonlinear wave loads on submerged decks in shallow water," *Journal of Fluids and Structures*, vol. 86, pp. 266–289, 2019.

[40] J. Humar, *Dynamics of structures*. CRC press, 2012.

[41] M. Hayatdavoodi and R. C. Ertekin, "Nonlinear wave loads on a submerged deck by the Green–Naghdi equations," *Journal of Offshore Mechanics and Arctic Engineering*, vol. 137, no. 1, 2015.